Elastic leak of a seal

Qihan Liu[1*], Zhengjin Wang[1,2*], Yucun Lou[3], Zhigang Suo[1 (a)]

[1]School of Engineering and Applied Sciences, Harvard University, Cambridge, MA 02138

[2] State Key Lab for Strength and Vibration of Mechanical Structures, International Center for Applied Mechanics, School of Aerospace Engineering, Xi'an Jiaotong University, Xi'an 710049, China

[3]Schlumberger-Doll Research, One Hampshire Street, Cambridge, MA 02139

*These authors contributed equally to this work.

(a) Email: suo@seas.harvard.edu

Abstract. An elastomeric seal may leak by elastic deformation without any material damage. We describe elastic leak using a theoretical model, and watch a seal deform and leak using a transparent experimental setup. The elastomer seals the fluid by forming contact with surrounding hard materials. As the fluid pressure increases, the contact stress also increases but not as much. When the fluid pressure surpasses the contact stress, the elastomer and the hard materials lose contact in some region, forming a leaking path. The critical fluid pressure for elastic leak depends on the geometry and constraint of the seal, but is insensitive to the rate at which the fluid is injected. Our study points to the significance of elastic deformation in modes of failure that also involve material damage.

Seals are ubiquitous. Familiar examples are those in plumbing joints, drinking bottles, and pressure cookers. Engines require seals to enable gas-tight, reciprocating motion of pistons in cylinders (Flitney 2007). Hydraulic fracture requires seals to isolate fluids in gaps between pipes and boreholes (Yakeley, Foster et al. 2007; Davis and McCrady 2008; Evers, Young et al. 2008; Mu, Ma et al. 2012). Seals, along with tires and bearings, are among the most significant applications of elastomers (Gent 2012). Seals are inexpensive, but their failure can be costly. The explosion of the space shuttle *Challenger*, for example, was traced to the failure of O-rings (Rogers, Armstrong et al. 1986).

The softness of an elastomer is essential to both the function and failure of a seal. The elastomer seals a fluid in a gap between mating parts made of hard materials. The softness enables the seal to deform easily, adapting to unpredictable variations in its working environment, such as the height of the gap, the misalignment of the mating parts, the roughness of their surfaces, and changes in temperature. With this adaptation, neither the seal nor the mating parts need to be designed with high precision, which could be costly or impossible. The softness of the elastomer, however, also makes the seal prone to failure. The fluid pressure can cause the seal to deform and damage, leading to leak (Nau 1987; Flitney 2007).

Here we study a particular mode of failure, elastic leak. An elastomer seals a fluid by forming contact with surrounding hard materials. As the fluid pressure increases, the contact stress also increases but not as much. When the fluid pressure surpasses the contact stress in some part of the contact region, the seal and the hard materials lose contact in this region, forming a leaking path which eventually penetrates through the whole contact region. This mode of failure is entirely due to elastic deformation: the seal leaks without any material damage. We construct a transparent experimental setup to watch the seal deform and leak, and compare experimental observations to theoretical predictions. We find that the critical fluid pressure for elastic leak depends on the geometry and constraint of the seal, but is insensitive to the rate at which the fluid is injected.

Whereas seals have been studied as boundary-value problems of elasticity (e.g., (George, Strozzi et al. 1987; Karaszkiewicz 1990; Nikas 2003), how the solutions of elasticity relate to the leak of seals is poorly understood. In postmortem examinations of failed seals, damage is often highly visible, but elastic deformation is not (Flitney 2007; Parker 2007). Perhaps because of this biased evidence, the central significance of elastic deformation to the leak of seals is underappreciated. The object of this paper is to quantify elastic leak using a combination of experiment and modeling.

A model of elastic leak. Prior to the injection of fluid, two rigid walls place an elastomer in a state of precompression (Fig. 1a). On the right side of the elastomer, a step in the bottom wall defines the sealing site. For the time being, we neglect the adhesion and friction between the walls and the elastomer, and assume that the elastomer deforms elastically without damage. The elastomer and the two walls form contact. We focus on the distribution of the contact stress between the elastomer and the top wall. The contact stress peaks in the interior of the contact, and vanishes at the edges of the contact (George, Strozzi et al. 1987).

When a fluid of a small pressure p is injected into the space on the left side of the seal, the elastomer deforms, pushes against the step, and extrudes a small part into the tight space above the step (Fig. 1b). The fluid pressure changes the region of contact, and increases and redistributes the contact stress (Karaszkiewicz 1990; Nikas 2003). When both the elastomer and the wall have smooth surfaces, the fluid pressure matches the contact stress at the edge of the contact. The edge of the contact would recede if the fluid pressure were above the contact stress at the edge of the contact, and would advance if the fluid pressure were below the contact stress at the edge of the contact. When the fluid pressure is low, the contact stress inside the contact rises above the fluid pressure. It is the rising contact stress in the interior of the contact that prevents the fluid from penetrating into the contact. The seal does not leak.

As the fluid pressure increases, the seal can fail in two modes. In one mode of failure, the whole elastomer squeezes into the tight space above the step, and escape from the sealing site (Eshel 1984)(Fig. 1c). Although the fluid pressure is still lower than the peak contact stress, the escaped seal is commonly considered a failure. This mode of failure, elastic escape, will not be studied in this paper. In the other mode of failure, as the fluid pressure increases, the peak contact stress also increases but not as much. When the fluid pressure reaches a critical value p_c, the contact stress peaks at the left edge of the contact and still matches the fluid pressure, whereas the contact stress in the interior of the contact drops below the fluid pressure (Fig. 1d). Consequently, the fluid penetrates the contact, pulled by the lower and lower contact stress ahead. The elastomer and the top wall lose contact in some region, forming a leaking path. This mode of failure, elastic leak, will be the focus of the remainder of the paper.
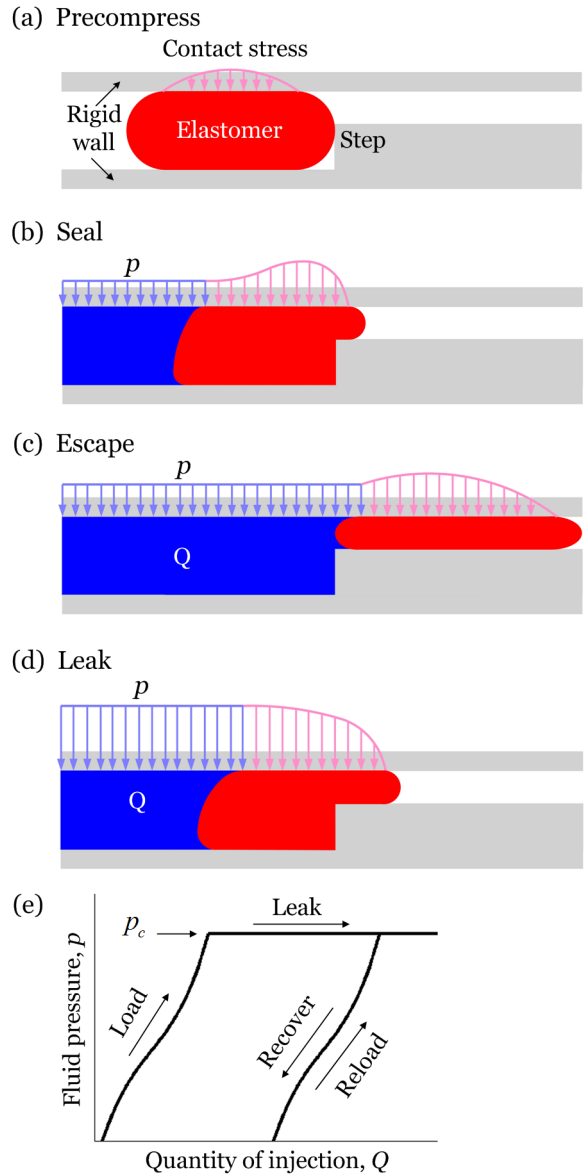
Figure 1. Elastic escape and elastic leak. (a) Prior to the injection of fluid, two rigid walls place an elastomer in a state of precompression. A step in the bottom wall defines the sealing site. Between the elastomer and the top wall is a distribution of contact stress. (b) When a fluid of quantity Q is injected, the fluid pressure p is applied on the elastomer and the elastomer deforms. The elastomer seals the gap when the contact stress rises above the fluid pressure. (c) The fluid pressure may cause the elastomer to squeeze into the tight space above the step, and escape from the sealing site. (d) The seal leaks when the contact stress in the interior of the contact drops below the fluid pressure. (e) A p-Q diagram characterizes elastic leak.

The seal is a nonlinear system. We use the fluid pressure p as the loading parameter, and use the quantity of injected fluid, Q, as a proxy for the state of the system. We characterize elastic leak using a p-Q diagram (Fig. 1e). As the quantity of injection Q increases, the fluid pressure p increases. When the fluid pressure reaches a critical level p_c, the seal leaks, and the quantity of injection can increase infinitely without increasing the fluid pressure. When the fluid pressure is reduced below the critical level, the leak stops, and the elastomer recovers toward its initial shape. When the fluid pressure is increased to p_c again, the leak resumes. Since we have assumed that the elastomer is elastic and the contact is free of adhesion and friction, the system is perfectly reversible. Whenever the leak stops, the seal has no memory of the previous leak. Each recovering-reloading curve parallels the initial loading curve, shifted by the quantity of fluid that has leaked through the seal.
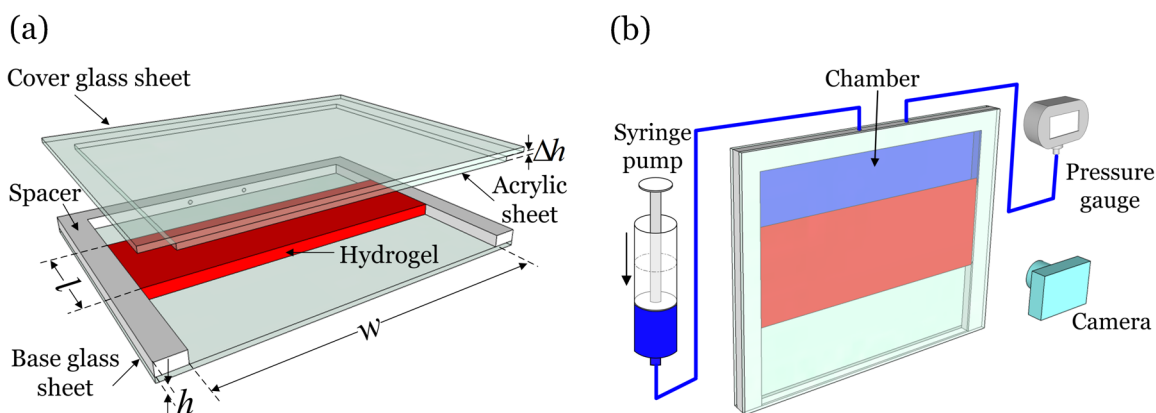

Figure 2. A desktop experimental setup. (a) The hydrogel, of dimensions h, l and w in the undeformed state, is glued to a sheet of glass and to acylic spacers. (b) An acrylic sheet of thickness Δh is attached to another sheet of glass. When the cover sheet is glued to the spacer, the hydrogel is precompressed with a displacement Δh. The glass, acrylic and hydrogel define a chamber, which connects to a syringe pump and a pressure gauge. The setup is placed vertically so that any leaked fluid can automatically drain out.

Experiment. The concept of elastic leak can be tested with any seal configuration. We study elastic leak with a desktop experiment. We use an adhesive to glue a layer of hydrogel, dimensions l, w and h, to acrylic spacers and a sheet of glass (Fig. 2a). A transparent acrylic sheet of thickness Δh and width w is attached to another sheet of glass, i.e. the cover glass sheet. When the cover glass sheet is glued on top of the acrylic spacers, the hydrogel is precompressed

with a strain $\varepsilon = \Delta h / h$ (Fig. 2b). No adhesive is applied between the cover sheet and the hydrogel. One side of the hydrogel is a sealed chamber, and the other side of the hydrogel is open to the air. We use a syringe pump to inject water into the chamber while a pressure gauge recordes the fluid pressure inside the chamber. A digital camera is used to monitor the movement of hydrogel and water, which are colored in red and blue. The setup is placed vertically during experiments so that any leaked fluid can automatically drain out. See a photo of the experimetal setup (Fig. S1).

Our experimental setup bears resemblance to seals commonly used in oilfields (Yakeley, Foster et al. 2007), but we design the setup with following considerations.   First, the transparency of the glass allows us to watch the seal deforming and leak. Second, the design ensures that the seal leaks before the glass breaks. For the fluid to deform the seal, the pressure in the fluid scales with the elastic modulus of the seal. To lower the pressure in the desktop experiment, we make the seal using a hydrogel of a low elastic modulus (~kPa), which is much below the elastic modulus of an elastomer (~MPa). Third, we design the seal to minimize the number of geometric parameters. We choose the rectangular shape with $w \gg h$, so that the aspect ratio l/h is the only dimensionless group describing the geometric effect of the seal. We prevent elastic escape not by a step in the bottom glass sheet, but by gluing the hydrogel to the bottom glass sheet. Fourth, the design allows us to vary the constraint of the seal by changing the strain of precompression, ε .

As the syringe pump injects fluid at a constant rate into the chamber, we measure the fluid pressure (Fig. 3a), and watch the seal deform and leak (Fig. 3b).   Initially, the fluid pressure rises, and the hydrogel deforms but does not leak. On reaching a peak value p_i , the fluid pressure drops precipitously, while a drop of water runs rapidly through the interface between the hydrogel and the cover sheet (Movie 1). The fluid pressure then settles at a plateau p_s , and the seal leaks in a steady state. When we remove the force applied to the syringe pump, immediately the fluid pressure drops below the plateau and the leak stops (Movie 2). It takes some time for the hydrogel to recover its initial configuration, and for the fluid pressure to vanish. No fracture or debris of hydrogels is observed.   We will call p_i the leak-initiation pressure, and p_s the leak-stop pressure. On pushing the syringe pump again at the constant rate of injection, we record a somewhat lower leak-initiation pressure, but nearly identical leak-stop pressure. The behavior of the seal is repeatable from cycle to cycle.
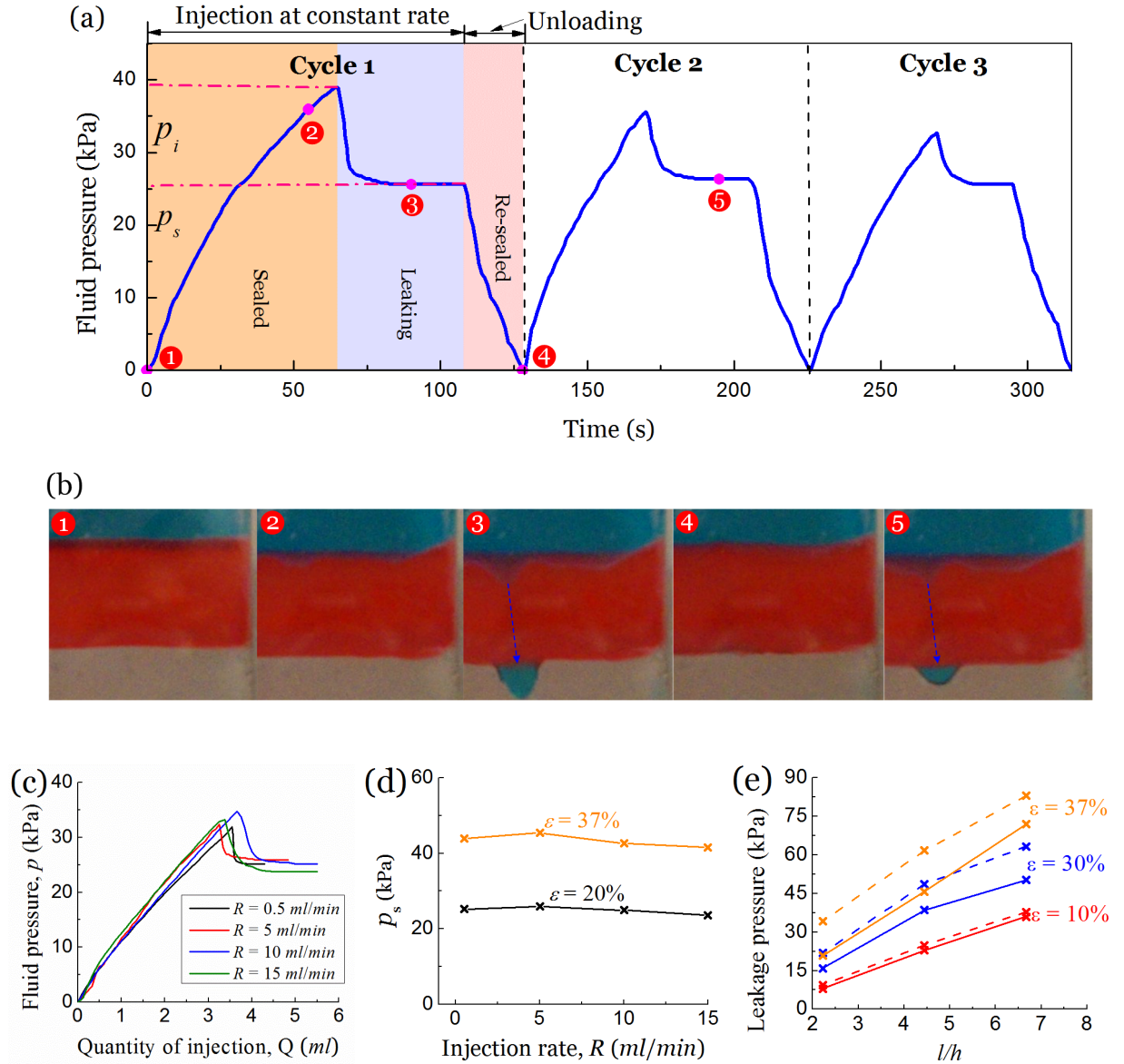
Figure 3. Experimental observations of elastic leak. (a) The fluid pressure as a function of time. A hydrogel, with shear modulus $\mu = 1.03\text{kPa}$, and dimensions h = 4.5 mm, l = 20 mm, and w = 120 mm, is precompressed at a strain of $\varepsilon = 20\%$. The syringe pump injects water at a rate of 5 ml/min until the seal leaks. After steady state leak is achieved the force applied on the syringe pump is removed. Three loading-unloading cycles are plotted. (b) Five snapshots of the seal correspond to states marked in the pressure-time curve in (a). (c) The p-Q curves at several rates of injection. (d) The leak-stop pressure is insensitive to the rate of injection, and increases with the strain of precompression. (e) The effects of the length to thickness ratio and the strain of precompression on the leak-initiation pressure (dashed lines) and leak-stop pressure (solid lines).

We conduct the experiment with several variables: the rate of injection, the strain of precompression, and the length of the seal. The *p-Q* diagram remains nearly identical even though the rate of injection changes by two orders of magnitude (Fig. 3c). The leak-stop pressure increses with the strain of precompression and with the length of the seal (Fig. 3d, 3e).

Comparision between the model and experiment. These experimental observations broadly confirm the model of elastic leak, but also show some significance differences. The model predicts that the leak initiates and stops at exactly the same pressure, p_c. The experiment, however, shows two distinct pressures: the peak (the leak-initiation pressure p_i), and the plateau (the leak-stop pressure p_s). This difference between the model and the experiment may result from friction between the hydrogel and the cover glass. Friction is neglected in the ideal model, but is present in the experiment. When the hydrogel deforms, additional fluid pressure is required to overcome the friction (Fig. S2). When the leak reaches steady state, however, the hydrogel stops deforming, and the additional fluid pressure to overcome friction is no longer necessary, so that a lower fluid pressure sustains the steady leak. We expect the seal during the steady leak to obey the elastic leak model, and p_s to be quantitatively comparable to the p_c. In particular, we expect p_s to depend only on the elastic and geometric properties of the system. Indeed, p_s is highly repeatable across cycles (Fig. 3a). By contrast, the leak-initiation is sensitive to friction. After the initial cycle, the friction may reduce if the interface between hydrogel and the glass traps water (Gong, Iwasaki et al. 1999). Consequently, subsequent cycles require lower leak-initiation pressures (Fig. 3a).

Our model predicts that, on reaching the critical pressure, the fluid faces monotonically decreasing contact stress (Fig. 1d). Thus, once the fluid enters the contact, it will unstably propagate through the entire contact. This behavior is indeed observed in experiment (Movie 1). The time scale for the unstable leak is very short comparing to the time scale of our experiment. This theoretical prediction explains why the fluid pressure drops precipitously after the seal starts to leak.

When a seal leaks, the fluid pressure keeps at a plateau pressure. This observation should not be surprising. There is not much resistance for the leaking path to spread, and the leaking path should be very thin so that the elastomer is only slightly perturbed from its configuration right before leak. The fluid pressure required to maintain the path is not much

higher than p_c, and is essentially unchanged when the rate of injection changes by two orders of magnitude.

Some variations in a seal are unavoidable, and the deformation is not perfectly uniform across the width of the hydrogel. The hydrogel and the cover glass lose contact in some region and form a leaking path. After the leak initiates, the fluid pressure drops, so that no other leaking path can form. In all experiments we observe only one leaking path in each seal. In the following cycles, the leaking path forms at the same place.

Computation. To compare the model and the experiment quantitatively, we analyze seals using the finite element software ABAQUS. The elastomer is modeled as an incompressible neo-Hookean material with shear modulus μ (Treloar 1975), and is assumed to deform under the plane strain conditions. The elastomer is a rectangular block in the undeformed state, bonded to the bottom wall, in contact with the top wall with neither adhesion nor friction. A precompression of strain ε is applied by lowering the top wall. The system has three dimensionless parameters: the normalized fluid pressure p/μ represents the load, the aspect ratio l/h represents the geometry of the seal, and the strain of precompression ε represents the constraint of the seal. At a given fluid pressure p/μ, we calculate the shape of the elastomer, and the distribution of the contact stress between the elastomer and the top wall (Fig. 4a-4d).

As noted before, when the two smooth surfaces form a contact, the contact stress at the edge of the contact matches the fluid pressure outside. This continuity, however, does not apply if either one of the two surfaces is not smooth (Johnson 1987). When the edge of the block of elastomer coincides with the edge of the contact, the contact stress at the edge of the contact in general differs from the fluid pressure.

In the absence of the fluid pressure, $p/\mu = 0$, the rigid walls place the elastomer in a state of precompression. Because the elastomer is bonded to the bottom wall and is in contact with the top wall with no friction and adhesion, the precompression causes the top part of the elastomer to bulge out. Small parts of the elastomer near its edges lose contact with the top wall—that is, the edges of the elastomer do not coincide with the edges of the contact. The contact stress is symmetrically distributed in the contact, peaks at the mid-point of the contact, and vanishes at the two edges of the contact.

At the fluid pressure of $p/\mu = 4.9$, the shape of the elastomer is asymmetric. At the right edge of the contact, additional area of the elastomer loses contact with the top wall, and the contact stress matches with the zero pressure outside. The left edge of the contact coincides with the edge of the elastomer, so that the contact stress does not match the fluid pressure. In

this case, the contact pressure at the left edge of the contact exceeds the fluid pressure, and the seal does not leak. The fluid pressure raises the contact stress, and shifts the peak contact stress toward the left edge.

At the fluid pressure of $p/\mu = 15.6$, the elastomer shears even more, and a significant amount of material extrude out at the right side. The distribution of contact stress becomes monotonic, peaks at the left edge of the contact, and vanishes at the right edge of the contact. The contact stress at the left edge remains above the fluid pressure, and the seal does not leak. This behavior persists up to the fluid pressure $p/\mu = 32.5$, when the peak contact stress matches the fluid pressure, and the seal leaks.

Following the above procedure, we calculate the critical fluid pressure for various values of l/h and ε using the finite element method, and fit our result to an analytical expression (Figs. S3, S4):

$$\frac{p_c}{\mu} = \frac{A}{1-\varepsilon}\left(\frac{l}{h}\right) + \frac{B\varepsilon}{1-\varepsilon}\left(\frac{l}{h}\right)^2,$$
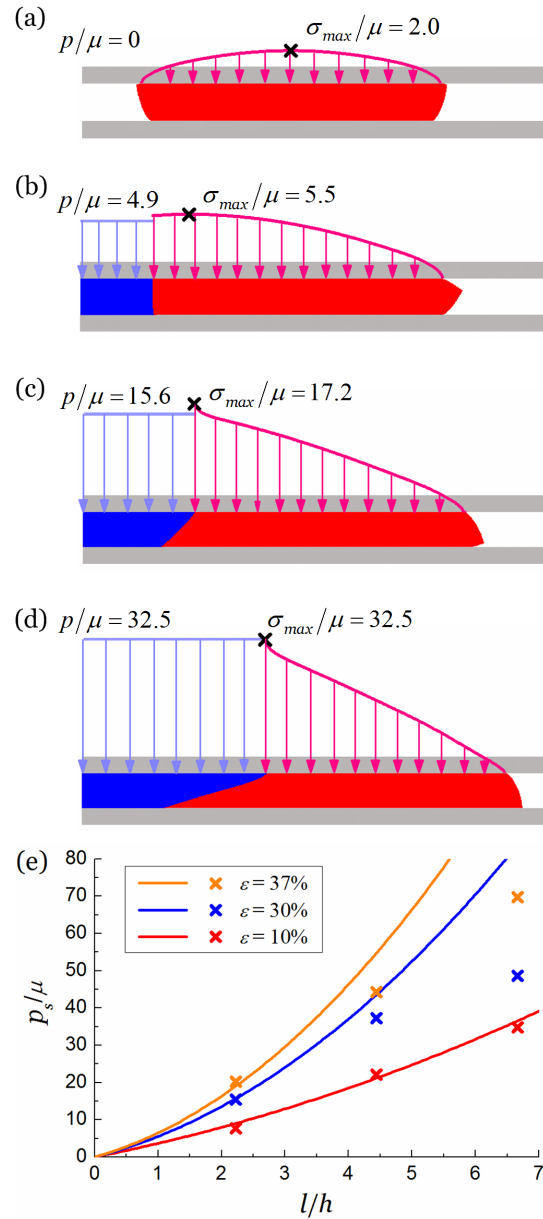(1)

with $A = 3.0$ and $B = 2.9$.

Figure 4. Finite element anaysis of elastic leak. (a)–(d) Snapshots of a deformed seal of rato $l/h = 6$ and a precompression $\varepsilon = 10\%$ at four levels of the fulid pressure. The corresponding distributions of contact stress are also plotted. At each level of the fluid pressure, a black cross marks the position of the peak contact stress. (e) The critical fluid pressure predicted theoretcally (solid curves) is compared with the leak-stop pressure measured experimentally (crosses).

We compare the theoretical predictions to the experimentally measured values of the leak-stop pressure (Fig. 4e). The agreement is good for low precompression $\varepsilon = 10\%$ or small ratios of l/h. For high precompression and large aspect ratios, the theoretical predictions and the experimental results differ, but they are still well within factor of two.

Figure 5. Elastic instability prior to the leak. (a) For a seal of low precompression ($\varepsilon = 10\%$, $l/h = 6.7$), prior to the leak, the edge of the hydrogel is nearly straight. (b) For a seal of moderate precompression ($\varepsilon = 30\%$) and a relatively small aspect ratio ($l/h = 2.2$), prior to the leak, the straight edge of the hydrogel becomes unstable and forms a wavy shape. (c) For a seal of high precompression ($\varepsilon = 37\%$) and a relatively large aspect ratio ($l/h = 4.4$), prior to the leak, the strainght edge of the hydogel becomes unstable but does not form a wavy shape.

The precise cause for the deviation between the theory and experiment is uncertain. One likely cause is the relaxation of the hydrogel. Prior to the injection of fluid, the hydrogel is in a state of precompression, and is stored for four hours to reach adequate adhesion. During this period, the contact stress due to precompression relaxes somewhat (Fig. S5). How this relaxation affects critical fluid pressure is a complex question, which we do not pursue here. Another likely cause is elastic instability prior to the leak. In a few cases, before the seal leaks, we observe that the straight edge of the hydrogel becomes unstable and forms a wavy shape (Fig. 5b, Movie 3). In some other cases, the pre-leak instability does not form waves, possibly because the ratio w/l is too small (Fig. 5c, Movie 4). The pre-leak instability violates the assumption of the plane strain conditions, and conceivably lowers the critical fluid pressure for elastic leak. However, our simulation based on the plane strain conditions gives good prediction for some cases where instability is observed. For example, for the case of distinct fingering instability (Fig. 5b, $\varepsilon = 30\%$, $l/h = 2.2$), the theoretical prediction agrees well with the experimentally measured critical pressure for elastic leak (Fig. 4e). A wavelike instability has been studied

recently for hydrogels bonded between two rigid walls (Biggins, Saintyves et al. 2013; Saintyves, Dauchot et al. 2013; Biggins, Wei et al. 2014), but the effect of this instability on elastic leak has not been studied.

Discussion. Elastic deformation is of central significance to the leak of seals. For instance, in oilfields elastomers are widely used to block fluids, e.g., for testing rocks (Weinheber and Vasques 2006), completing boreholes (Noguera, Sierra et al. 2009), and preparing boreholes for multi-stage hydraulic fracture (Mu, Ma et al. 2012). In contrast to many other applications, the sealing conditions in oilfields cannot be fully determined before operation. Seals may be insufficiently constrained due to the uncertainty of the sizes of boreholes, unexpected damage of the gauge rings, and insufficient swelling of the elastomers (Lou, Robisson et al. 2012). Such seals can leak without appreciable damage of the elastomer (Nijhof, Koloy et al. 2010).

Even for seals subject to high constraint, where failure is commonly attributed to the damage of elastomers (Nau 1999; Flitney 2007), damage by itself often does not create a leaking path. Rather, damage is a precursor for leak, lowering the constraint, allowing the seal to undergo excessive elastic deformation. Examples include fracture and abrasion of the elastomer, and debonding between the elastomer and the rigid walls. After a certain amount of damage, the seal leaks by the elastic deformation of the leftover material. In some cases over 50% of the material is lost before the seal leaks (Parker 2007). A seal can also fail because the properties of elastomer change with time. The elastomer may become brittle due to aging, or soften because crosslinks break down, or develop irreversible deformation due to the formation of crosslinks under heat and chemical attack, or swell in the presence of solvent (Flitney 2007). In most cases, a seal still leaks by forming a leaking path in the contact with the hard materials. That is, elastic leak follows degradation.

In summary, we study elastic leak, a mode of failure in which seals leak by elastic deformation without any material damage. We design an experiment to watch seals deform and leak, and compare experimental observations with theoretical predictions. We find that the critical fluid pressure for elastic leak depends on the geometry and constraint of the seal, but not on the rate at which the fluid is injected. Our study points to the significance of elastic deformation in modes of failure that also involve material damage.

Fabrication of seals. We synthesize polyacrylamide hydrogel using the free-radical method. Acrylamide (AAM), N,N'-methylenebis(acrylamide) (MBAA), ammonium persulfate (APS) and N,N,N',N'-tetramethylethylenediamine (TEMED) are acquired from Sigma Aldrich. We dissolve powder of AAM in deionized water with the weight fraction of AAM fixed at 0.12

that of the aqueous solution. We add MBAA (at 0.0006 the weight of AAM) as the crosslinker, TEMED (at 0.0025 the weight of AAM) as the crosslinker accelerator, and APS (at 0.0085 the weight of AAM) as initiator for free-radical polymerization. We color the hydrogel in red using a food dye (Shank's Extracts, acquired from VWR International LLC.), at 0.002 the volume of aqueous solution. We pour the solution into plastic molds to form rectangular samples. After gelation, the samples are stored at room temperature for 1 day to complete polymerization. We glue the hydrogel to acrylic spacers and the glass using superglue (Loctite® Instant-Bonding Adhesive 409, acquired from McMaster-CARR). We store the sealed setup in a humid box for 4 hours to reach sufficient adhesion. We color water in blue using a food dye (Shank's Extracts, acquired from VWR International LLC.).

Finite element analysis. We use the finite element software ABAQUS, and model the elastomer with the CPE4H element. We prescribe the bottom boundary of the elastomer with zero displacement, and allow all the other boundaries of the elastomer to form frictionless contact with the rigid walls. The contact is enforced with the augmented Lagrange method. The top wall is moved downward to apply the precompression. Uniform pressure is applied on the left boundary of the elastomer. When the strain precompression is greater than 20%, the top left tip will reach critical strain for the onset of a crease. To avoid this instability, a rounded corner with a radius of 1% of the sample thickness is added. This defect affects the contact stress somewhat and reduces p_c by a small amount. To ease difficulty in simulating contact, for large aspect ratio and high precompression cases, the left portion of the top boundary that is expected to be in contact with the top wall has been applied with a sliding boundary condition instead of the contact condition. In all these cases, this part of the boundary is under compression, and will not detach from the wall.

References

Biggins, J. S., B. Saintyves, et al. (2013). "Digital instability of a confined elastic meniscus." Proceedings of the National Academy of Sciences.

Biggins, J. S., Z. Wei, et al. (2014). "Fluid driven fingering instability of a confined elastic meniscus." arXiv:1407.0684v2 [cond-mat.soft].

Davis, T. W. and D. D. McCrady (2008). Using Swellable Packers To Provide Annular Isolation for Multistage Fracture Treatments. <u>SPE Annual Technical Conference and Exhibition</u>. Denver, Colorado, USA, Society of Petroleum Engineers.

Eshel, R. (1984). "Prediction of Extrusion Failures of O-Ring Seals." <u>A S L E Transactions</u> **27**(4): 332-340.

Evers, R., D. Young, et al. (2008). Design Methodology for Swellable Elastomer Packers (SEPs) in Fracturing Operations. <u>SPE Annual Technical Conference and Exhibition</u>. Denver, Colorado, USA, Society of Petroleum Engineers.

Flitney, R. (2007). Seals and Sealing Handbook. R. Flitney. Oxford, Elsevier Science.

Gent, A. N. (2012). <u>Engineering with Rubber(Third Edition)</u>, Hanser.

George, A. F., A. Strozzi, et al. (1987). "Stress fields in a compressed unconstrained elastomeric O-ring seal and a comparison of computer predictions and experimental results." <u>Tribology International</u> **20**(5): 237-247.

Gong, J., Y. Iwasaki, et al. (1999). "Friction of Gels. 3. Friction on Solid Surfaces." <u>The Journal of Physical Chemistry B</u> **103**(29): 6001-6006.

Johnson, K. L. (1987). <u>Contact Mechanics</u>. New York, Cambridge University Press.

Karaszkiewicz, A. (1990). "Geometry and contact pressure of an O-ring mounted in a seal groove." <u>Industrial & Engineering Chemistry Research</u> **29**(10): 2134-2137.

Lou, Y., A. Robisson, et al. (2012). "Swellable elastomers under constraint." <u>Journal of Applied Physics</u> **112**(3): 034906-034906-034906.

Mu, L., X. Ma, et al. (2012). Evaluation of Multi-stage Fracturing by Hydrajet, Swellable Packer, and Compressive Packer Techniques in Horizontal Openhole Wells. <u>SPE Europec/EAGE Annual Conference</u>. Copenhagen, Denmark, Society of Petroleum Engineers.

Nau, B. S. (1987). "The State of the Art of Rubber-Seal Technology." <u>Rubber Chemistry and Technology</u> **60**(3): 381-416.

Nau, B. S. (1999). "An historical review of studies of polymeric seals in reciprocating hydraulic systems." <u>Proceedings of the Institution of Mechanical Engineers, Part J: Journal of Engineering Tribology</u> **213**(3): 215-226.

Nijhof, J., T. R. Koloy, et al. (2010). Valhall - Pushing the limits for Open Hole Zonal Isolation - qualification and field trial of 10.000 psi oil swelling packers. <u>SPE EUROPEC/EAGE Annual Conference and Exhibition</u>. Barcelona, Spain, Society of Petroleum Engineers.

Nikas, G. K. (2003). "Analytical study of the extrusion of rectangular elastomeric seals for linear hydraulic actuators." <u>Proceedings of the Institution of Mechanical Engineers, Part J: Journal of Engineering Tribology</u> **217**(5): 365-373.

Noguera, J. A., L. Sierra, et al. (2009). First Coiled Tubing Swellable-Packer Deployment in the Middle East. <u>SPE/ICoTA Coiled Tubing & Well Intervention Conference and Exhibition</u>. The Woodlands, Texas, Society of Petroleum Engineers.

Parker (2007). Packer O-Ring Handbook - ORD5700. Cleveland, OH, USA, Parker Hannifin Corporation**:** p. 253.

Rogers, W. P., N. A. Armstrong, et al. (1986). Report of the Presidential Commission on the Space Shuttle Challenger Accident, Chapter IV: The Cause of the Accident. R. Commission.

Saintyves, B., O. Dauchot, et al. (2013). "Bulk Elastic Fingering Instability in Hele-Shaw Cells." <u>Physical Review Letters</u> **111**(4): 047801.

Treloar, L. R. G. (1975). <u>The Physics of Rubber Elasticity (Third Edition)</u>, Oxford: Clarendon Press.

Weinheber, P. and R. Vasques (2006). New Formation Tester Probe Design for Low Contamination Sampling. <u>SPWLA 47th Annual Logging Symposium</u>. Veracruz, Mexico, Society of Petrophysicists and Well-Log Analysts.

Yakeley, S., T. Foster, et al. (2007). Swellable Packers for Well Fracturing and Stimulation. <u>SPE Annual Technical Conference and Exhibition</u>. Anaheim, California, U.S.A., Society of Petroleum Engineers.